Hindawi
Journal of Sensors
Volume 2019, Article ID 1354029, 7 pages
https://doi.org/10.1155/2019/1354029

Research Article

A High Precision Fiber Bragg Grating Inclination Sensor for Slope Monitoring

Hongbin Xu[1], **Feng Li**[2], **Weigang Zhao**[3], **Shupeng Wang**[2], **Yanliang Du**[3] and **Ce Bian**[3]

[1]*School of Civil Engineering, Beijing Jiaotong University, Beijing 100044, China*
[2]*School of Civil Engineering, Wuhan University, Wuhan 430074, China*
[3]*Structure Health Monitoring and Control Institute, Shijiazhuang Tiedao University, Shijiazhuang 050043, China*

Correspondence should be addressed to Hongbin Xu; xuhongbin@semi.ac.cn

Received 15 March 2019; Revised 24 May 2019; Accepted 3 June 2019; Published 24 June 2019

Academic Editor: Carlos Marques

A high precision and small size Fiber Bragg Grating (FBG) inclination sensor which is used for slope monitoring is proposed in this paper. The FBG inclination sensor has a pendulum structure for high precision and a circular body for easy installation in the common inclinometer pipe. The sensitivity of the FBG inclination sensor can reach 400 pm/deg by optimizing its parameters. The test results show the superior performance of this FBG inclination sensor in terms of static characteristics, and its sensitivity is 406.6 pm/deg. The comparison experiment shows the static characteristics of the FBG inclination sensor are better than the traditional electrical inclination sensor.

1. Introduction

Slope engineering is common in mountain airport, railway, and highway traffic [1]. China is now developing the infrastructure fast; the number of the slopes is growing fast. However, landslides often happen in areas of poor geological conditions [2], which seriously threatens the safety of traffic facilities and people.

Deformation monitoring of the slope is very significant to knowing a slope's status and trend and carrying out evaluation and geological disaster warning [3]. Traditional slope monitoring technologies often use electromagnetic sensors [4] and acquisition instruments [5], where an electrical signal is highly susceptible to electromagnetic interference [6] and cannot be transmitted over a long distance. Large-scale slope monitoring cannot be achieved by traditional slope monitoring technologies.

With the optical fiber sensing technology having achieved rapid progress, its application in slope internal displacement monitoring has attracted a lot of attention [7–10]. Compared with the electrical sensing monitoring technology, it has strong corrosion resistance, strong antielectromagnetic interference, ease of composite network, long distance transmission, and other obvious advantages [11]. These advantages make it very suitable for remotely monitoring a large-scale slope engineering under a harsh environment. However, at present, most of the FBG inclination sensors are either with insensitivity [12, 13] or with large size [14], meaning they are unable to meet the needs of slope monitoring.

An FBG inclination sensor with high precision and small size was designed in this paper. The FBG inclination sensor has a pendulum structure and a circular body for high precision and easy installation in the inclinometer pipe; the sensitivity can reach 406.6 pm/deg and is much higher than that of the current FBG inclination sensor; it is with a small size which is suitable for most of the inclinometer pipe. The experimental results show that the FBG inclination sensor's main static performance specifications are good, and the shape of the external part meets the demand of the engineering.

2. Sensor Design and Analysis

2.1. Structural Design. The FBG inclination sensor that has a pendulum structure and a circular body for high precision

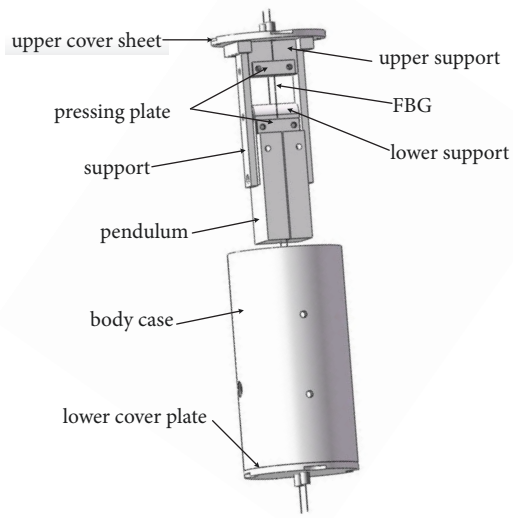

Figure 1: The structure diagram of the FBG inclination sensor.

and easy installation in the inclinometer pipe was designed in this paper, as shown in Figure 1. The FBG inclination sensor consists of the upper cover sheet, body case, upper support, support, pressing plate, lower support, pendulum, lower cover sheet, FBG, etc.

Each part of the FBG inclination sensor is made of 304 stainless steel material with strong corrosion resistance, except the pendulum structure which is a key influence factor of the sensitivity of the FBG inclination sensor, and the lead is selected as its material. The above parts of the FBG inclination sensor are connected by screws; in order to reduce the friction force between the low support and the support, two ball bearings are installed between them.

One end of the two FBGs is fixed on the upper support through a pressing plate by screws, and the other end of the two FBGs is fixed on the lower support in the same way. A certain amount of prestress is applied on both FBGs during the encapsulation; when the FBG inclination sensor is tilted, the prestress of one of the FBGs is increased while the prestress of the other FBG is released, and the center wavelength of the FBG shifts as the prestress changes. Therefore the tilt angle of the inclinometer pipe can be monitored by measuring the wavelength shift of the FBG by establishing the relationship between the tilt angle of the FBG inclination sensor and the wavelength shift of the FBG.

The influence of environment temperature cannot be neglected as the FBG has a high temperature sensitivity, but using the differential compensation design can achieve temperature compensation as the two FBGs have the same temperature coefficient; meanwhile, the FBG inclination sensors will have double sensitivity by the proposed structure [15].

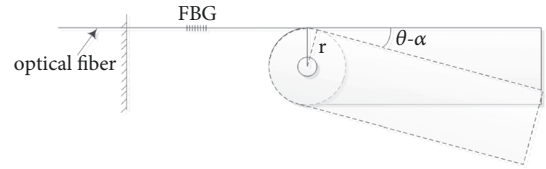

Figure 2: Schematic diagram of optical fiber stretching.

2.2. Theory Analysis. The component of the gravity of the pendulum provides the tensile force of the FBG. When the angle between the vertical direction and the pendulum is α, the tensile force of the FBG is

$$F = \frac{r' G \sin\alpha}{r} = \frac{r' G \alpha}{r}, \tag{1}$$

where F refers to the tensile force of the FBG provided by the component of the gravity of the pendulum; G refers to the gravity of the pendulum; α refers to the angle between the pendulum and vertical direction; r refers to the turning radius of the optical fiber; r' refers to the turning radius of the pendulum.

For FBG,

$$\varepsilon = \frac{\sigma}{E} = \frac{F}{\pi R^2 E} = \frac{\Delta l}{l}, \tag{2}$$

where σ refers to the strain of the FBG; E refers to the elastic modulus of the FBG; R refers to the radius of the FBG; l refers to the length of the stressed part of the optical fiber between the upper support and the lower support; $\triangle l$ refers to the stretched length of the optical fiber with a length of l.

The stretched length of the optical fiber under force F is equal to the arc length of the relative rotation angle, as shown in Figure 2, and the arc length formula is as shown in

$$\Delta l = r(\theta - \alpha), \tag{3}$$

where θ refers to the deflection angle of the FBG inclination sensor (inclinometer); α refers to the angle between the pendulum and the vertical direction when the deflection angle of the FBG inclination sensor is θ.

As can be seen from the above equation,

$$\alpha = \frac{\pi r^2 E R^2}{\pi r^2 E R^2 + l r' G}\theta. \tag{4}$$

The relationship between the center wavelength and the strain of FBG is as follows [16]:

$$\frac{\Delta\lambda}{\lambda} = (1 - P_e)\varepsilon, \tag{5}$$

where $\Delta\lambda$ refers to the variable quantity of the central wavelength of the FBG; λ refers to the center wavelength of the FBG; P_e refers to the elastic-optical coefficient of the FBG.

The sensitivity of the FBG inclination sensor is

$$S = \frac{\Delta\lambda}{\theta} = (1 - P_e)\lambda \frac{G r r'}{\pi r^2 E R^2 + l r' G}. \tag{6}$$

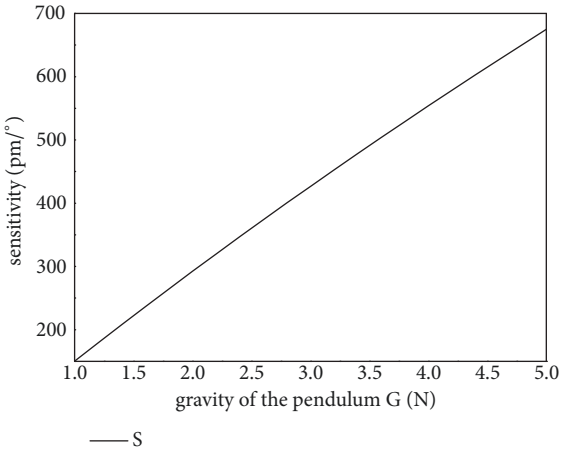

Figure 3: The relationship between *G* and *S*.

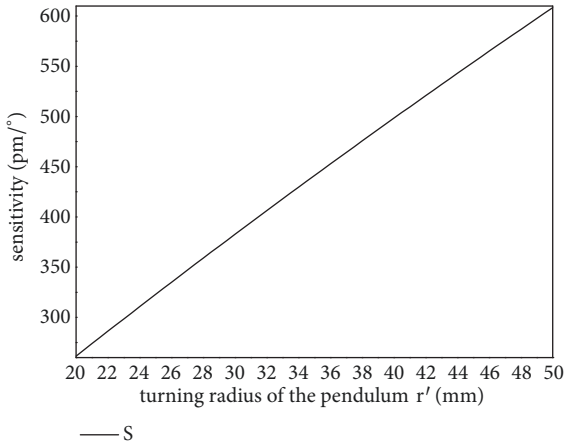

Figure 5: The relationship between *r*' and *S*.

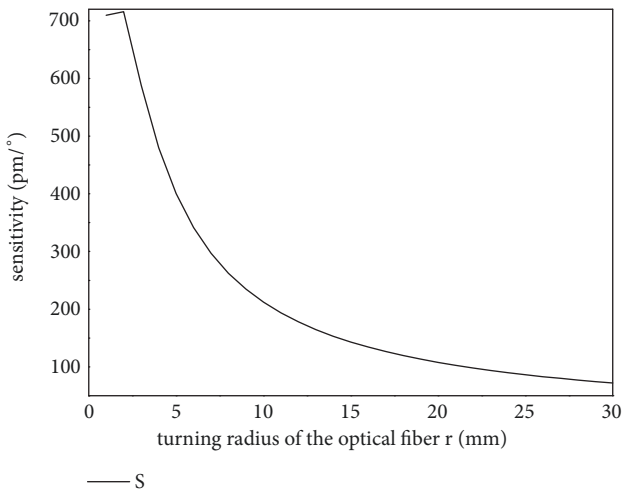

Figure 4: The relationship between *r* and *S*.

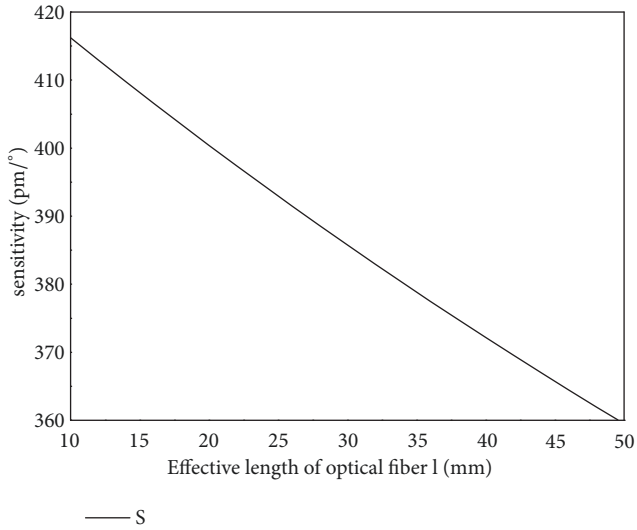

Figure 6: The relationship between *l* and *S*.

According to formula (6), the relationship between *G*, *r*, *r*', *l*, and *S* can be shown in Figures 3–6. *S* obviously has positive correlation with *G*, *r*' and negative correlation with *r*, *l*. Increasing *G* and *r*' can improve the sensitivity of the FBG inclination sensor, but it is not conducive to the miniaturization of the FBG inclination sensor; reducing *r* and *l* can improve the sensitivity of the sensor, but it is not conducive to the encapsulation of the sensor. The parameters of the FBG inclination sensor are gotten by optimization as shown in Table 1.

3. Test of the Main Static Performance

According to the Calibration Specification for Angular-Position Transducers/Sensor (JJF 1352-2012) and Methods for Calculating the Main Static Performance Specifications of Transducers (GB/T 18459-2001), the static characteristics of the FBG inclination sensor, such as sensitivity, hysteresis, repeatability, and linearity, were tested.

A SM125 FBG interrogator manufactured by MOI Company (America) and a KSMG15-65 angular-position system manufactured by Zolix (China) were adopted for static characteristics tests of the FBG inclination sensor, as shown in Figure 7.

The test step length of the FBG inclination sensor is 0.5° and the span is -3° to -3°. Three round trips of up-travel and down-travel are tested totally; the test result of the FBG inclination sensor is shown in Figures 8 and 9.

The measuring range of the proposed FBG inclination sensor is -3° ~ 3° and the span of the proposed FBG inclination sensor is 6°.

Sensitivity is the variable quantity of the FBG's center wavelength of the FBG inclination sensor caused by the unit angle input. So the sensitivity of the FBG inclination sensor can be defined as

$$\lim_{x \longrightarrow 0} \left(\frac{Y}{X} \right) = \frac{dY}{dX}, \tag{7}$$

Table 1: Materials and parameters of the FBG inclination sensor.

Name	Parameter	Material
Effective length of optical fiber l	20 mm	Quartz
Optical fiber (FBG) radius R	0.0625 mm	
Optical fiber (FBG) elastic modulus E	70 Gpa	
Pendulum volume	22×24×47 mm	Lead
Pendulum gravity G	2.8 N	
The turning radius of the optical fiber r	5 mm	
The turning radius of the pendulum r'	31.5 mm	
FBG inclination sensor length	90 mm	Stainless steel
The theoretic sensitivity of the FBG inclination sensor S	400.4 pm/∘	

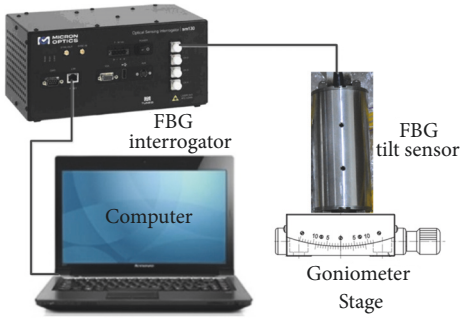

Figure 7: The static characteristics test system of the FBG inclination sensor.

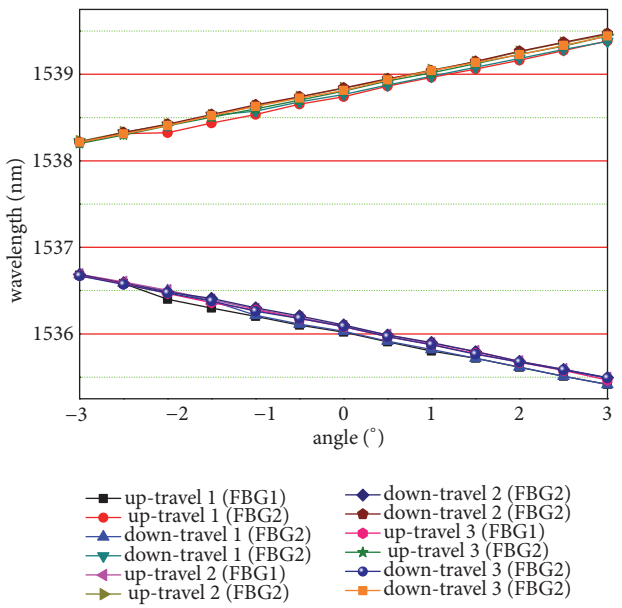

Figure 8: The test result of the FBG inclination sensor with three round trips.

where dY refers to the drift of center wavelength difference of the two FBGs of the FBG inclination sensor; dX refers to the input angle of the FBG inclination sensor.

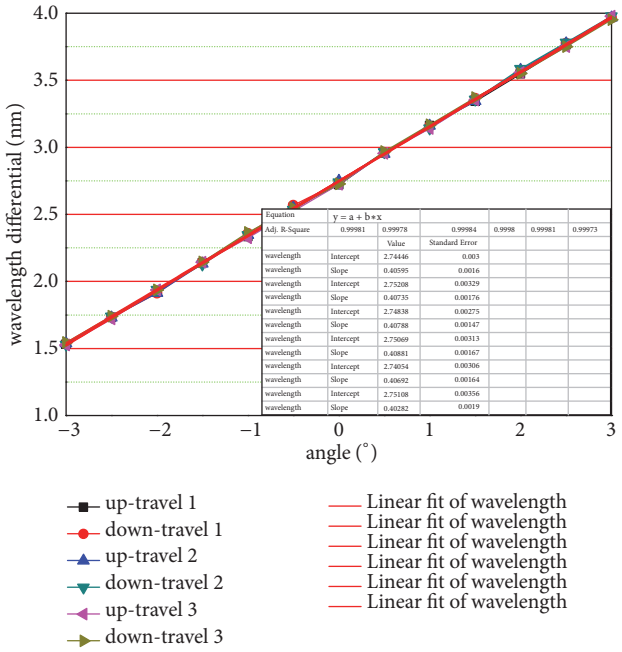

Figure 9: The analysis of the test result of the FBG inclination sensor.

The test results accord with the data curves of least squares; the average sensitivity of the designed FBG inclination sensor is about 406.6 pm/deg with a linear fitting of 0.999.

Resolution is the minimum variable quantity that can be detected in the measured value by the FBG inclination sensor. The designed FBG inclination sensor has a resolution of 8.9" considering the 1 pm accuracy of FBG interrogator.

Linearity is the error between the measured value and the theoretical value; it is generally adopted:

$$\xi_L = \frac{\left|\overline{y_i} - y_i\right|_{\max}}{y_{\max} - y_{\min}} \times 100\%, \tag{8}$$

where $\overline{y_i}$ refers to the average value of the output quantity of the sensor at the test point; y_i refers to the theoretical value of the fitting line; y_{max} refers to the average value of the maximum output quantity of the three cyclics; y_{min} refers

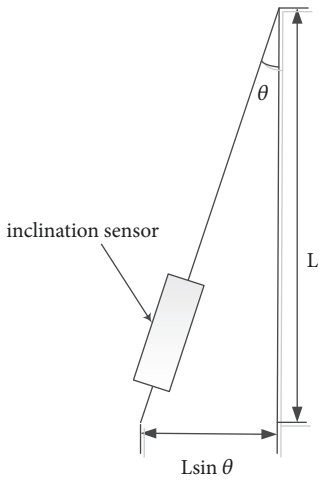

Figure 10: The principle of the indoor experiment.

to the average of the minimum output quantity of the three cyclics.

The linearity of the proposed FBG inclination sensor is 0.62%.

Hysteresis is the difference between the output quantity of the FBG inclination sensor in the up-travel and the output quantity of the FBG inclination sensor in the same input quantity of the down-travel, and it can be defined as

$$\xi_H = \frac{y_{Hmax}}{y_{max} - y_{min}} \times 100\%, \quad (9)$$

where y_{Hmax} refers to the maximum difference output quantity between the up-travel and the down-travel in the same input quantity of the FBG inclination sensor.

The hysteresis of the proposed FBG inclination sensor in this paper is 0.86%.

The output quantity of the FBG inclination sensor in three cyclics is different from each cyclic in the same input quantity, which is called repeatability, defined as

$$\xi_R = \frac{0.61\Delta_i}{y_{max} - y_{min}} \times 100\%, \quad (10)$$

where $\triangle_i$ refers to the largest difference of the output quantity of the FBG inclination sensor in the three cyclics in the same input quantity.

The test results show the repeatability of the FBG inclination sensor is 0.85%.

4. Indoor Simulation Experiment

In order to compare the performance of the FBG inclination sensor with that of the traditional electrical inclination sensor, an indoor simulation experiment was carried out. The experiment principle is as shown in Figure 10 and the testing photo is shown in Figure 11. The experiment equipment mainly consists of an inclinometer pipe, an FBG inclination sensor, a traditional electrical inclination sensor, a dial indicator, a SM125 FBG interrogator, and a voltage collector. The electrical inclination sensor is manufactured by Wuhan Jishen Angle Measuring Instrument Co., Ltd., the SM125 FBG interrogator is manufactured by Micron Optics, Inc., and the voltage collector is manufactured by the Institute of Semiconductors of the Chinese Academy of Sciences.

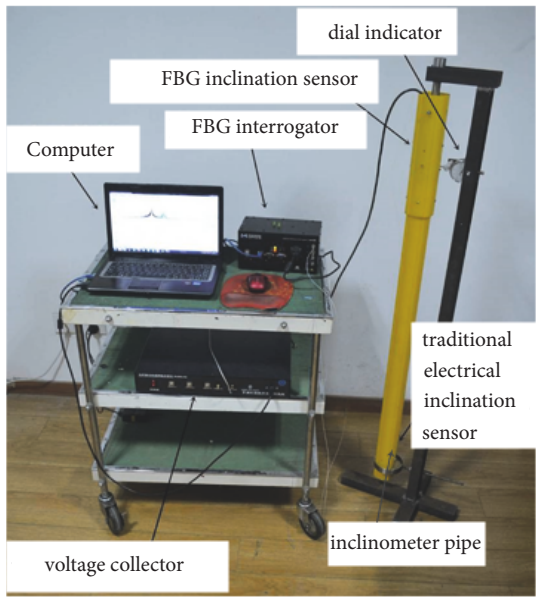

Figure 11: Photo of indoor simulation test.

Use predesigned support to suspend the inclinometer pipe. The displacement of the inclinometer pipe is recorded by a dial indicator. Both the FBG inclination sensor and traditional electrical inclination sensor are installed in the inclinometer pipe; the installation method is as shown in Figure 12. The FBG inclination sensor is demodulated with the FBG interrogator and the traditional electrical inclination sensor collected by the voltage collector. The testing process is also according to the Calibration Specification for Angular-Position Transducers/Sensor (JJF 1352-2012) and Methods for Calculating the Main Static Performance Specifications of Transducers (GB/T 18459-2001), and the test results are shown in Table 2. The test results have shown that the static characteristics of the FBG inclination sensor are much better than those of the traditional electrical inclination sensor.

5. Conclusions

In this paper, a high precision and small size Fiber Bragg Grating (FBG) inclination sensor was proposed; the FBG inclination sensor has a pendulum structure with a high sensitivity of 406.6 pm/deg and a circular body for ease of installation in the common inclinometer pipe.

In this paper, the theoretical analysis and the static calibration of the FBG inclination sensor were done. The measuring sensitivity of the FBG inclination sensor was exactly like the theoretic sensitivity, and the experimental results showed the static characteristics of the FBG inclination sensor are better than those of the traditional electrical inclination sensor, and the static characteristics of the FBG inclination

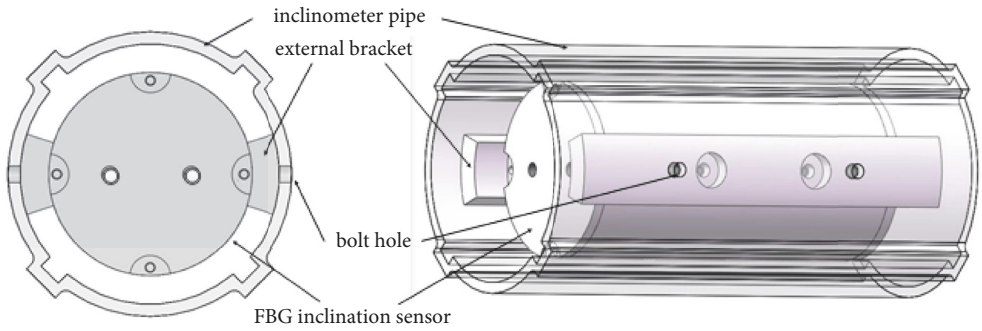

Figure 12: The installation method of the FBG inclination sensor.

Table 2: The rest of the indoor simulation experiment.

Sensor type	Linearity	Hysteresis	Repeatability
FBG inclination sensor	0.8%	0.92%	1.1%
Traditional electrical inclination sensor	1.52%	1.03%	1.38%

sensor were as follows: hysteresis 0.86%, repeatability 0.85%, and linearity 0.62%.

The indoor simulation experiment shows that the FBG inclination sensor is effective and significant in practical application, especially in the field of slope slip monitoring.

Data Availability

The data used to support the findings of this study are available from the corresponding author upon request.

Conflicts of Interest

The authors declare that they have no conflicts of interest regarding the publication of this paper.

Acknowledgments

This work was supported by the National Natural Science Foundation of China (No. 51578349, No. 51608336), the Scientific Research Project of Education Department in Hebei Province (No. QN2018239), the Science and Technology Plan Projects of Tibet (No. XZ201801-GB-07), and the Natural Science Foundation in Hebei Province (No. 2019210214).

References

[1] X. Yang, Y. Zhu, Y. Zhou, X. Yang, and Z. Shi, "Time-space monitoring and stability analysis of high fill slope slip process at a airport in mountain region," *Chinese Journal of Rock Mechanics & Engineering*, vol. 35, no. A2, pp. 3977–3990, 2016.

[2] C. Tseng, Y. Chan, C. Jeng, and Y. Hsieh, "Slip monitoring of a dip-slope and runout simulation by the discrete element method: a case study at the Huafan University campus in northern Taiwan," *Natural Hazards*, vol. 89, no. 3, pp. 1–21, 2017.

[3] T. Uchimura, I. Towhata, L. Wang et al., "Precaution and early warning of surface failure of slopes using tilt sensors," *Soils and Foundations*, vol. 55, no. 5, pp. 1086–1099, 2015.

[4] J. S. Marciano Jr., M. A. H. Zarco, M. C. R. Talampas et al., "Real-world deployment of a locally-developed tilt and moisture sensor for landslide monitoring in the Philippines," in *Proceedings of the 2011 IEEE Global Humanitarian Technology Conference, GHTC 2011*, pp. 344–349, USA, November 2011.

[5] J. S. Marciano, C. G. Hilario, M. A. B. Zabanal et al., "Monitoring system for deep-seated landslides using locally-developed tilt and moisture sensors: System improvements and experiences from real world deployment," in *Proceedings of the 4th IEEE Global Humanitarian Technology Conference, GHTC 2014*, pp. 263–270, USA, October 2014.

[6] W. Huang, W. Zhang, and F. Li, "Acoustic emission source location using a distributed feedback fiber laser rosette," *Sensors*, vol. 13, no. 10, pp. 14041–14054, 2013.

[7] H. Pei F, J. Yin H, and W. Jin, "Development of novel optical fiber sensors for measuring tilts and displacements of geotechnical structures," *Measurement Science & Technology*, vol. 24, no. 9, Article ID 095202, 2013.

[8] F. Li, W. Zhang, F. Li, and Y. Du, "Fiber optic inclinometer for landslide monitoring," *Applied Mechanics and Materials*, vol. 166-169, pp. 2623–2626, 2012.

[9] Y. Sun, B. Shi, D. Zhang, H. Tong, G. Wei, and H. Xu, "Internal deformation monitoring of slope based on BOTDR," *Journal of Sensors*, vol. 2016, 2016.

[10] F. Li, W. Zhao, H. Xu, S. Wang, and Y. Du, "A highly integrated BOTDA/XFG sensor on a single fiber for simultaneous multi-parameter monitoring of slopes," *Sensors*, vol. 19, no. 9, Article ID 2132, 2019.

[11] W. Huang, W. Zhang, Y. Luo, L. Li, W. Liu, and F. Li, "Broadband FBG resonator seismometer: principle, key technique, self-noise, and seismic response analysis," *Optics Express*, vol. 26, no. 8, pp. 10705–10715, 2018.

[12] H. Bao, X. Dong, H. Gong et al., "Temperature-insensitive FBG tilt sensor with a large measurement range," *Communications and Photonics Conference and Exhibition*, pp. 1-2.

[13] P. C. Peng Cui, W. Z. Wentao Zhang, and Y. S. Ying Song, "High resolution inclinometer based on vertical pendulum and fiber Bragg grating Fabry–Perot cavity," *Chinese Optics Letters*, vol. 16, no. 11, Article ID 110603, 2018.

[14] H. Y. Au, S. K. Khijwania, H. Y. Fu, W. H. Chung, and H. Y. Tam, "Temperature-insensitive fiber bragg grating based tilt sensor with large dynamic range," *Journal of Lightwave Technology*, vol. 29, no. 11, Article ID 5740549, pp. 1714–1720, 2011.

[15] M. Yang, D. Wang, Y. Rao et al., "Fiber optic displacement sensor used in railway turnout contact monitoring system," in *Proceedings of the Asia Pacific Optical Sensors Conference 2013*, Wuhan, China.

[16] Guo. H-Y, Z-B. Wang, and H-Y. Li, "Development and commissioning of high temperature fbg solid pressure sensors," *Journal of Sensors*, vol. 2018, Article ID 2056452, 8 pages, 2018.